International Journal of Modern Physics A

EVOLUTION OF THE STRUCTURE FACTORS IN PURE SU(N) LATTICE GAUGE THEORY AND EFFECTIVE SPIN MODELS

ALEXEI BAZAVOV, BERND A. BERG
and ALEXANDER VELYTSKY *

Department of Physics, Florida State University
Tallahassee, FL 32306-4350, USA
School of Computational Science, Florida State University
Tallahassee, FL 32306-4120, USA

Received 1 November 2004

We consider model A dynamics for a quench from the disordered into the ordered phase of SU(3) lattice gauge theory and the analogue $3d$ 3-state Potts model. For the gauge model this corresponds to a rapid heating from the confined to the deconfined phase. The exponential growth factors of low-lying structure function modes are numerically calculated. The linear theory of spinodal decomposition is used to determine the critical modes. This allows for the Debye screening mass estimation in an effective phenomenological model. The quench leads to competing vacuum domains, which make the equilibration of the QCD vacuum after the heating non-trivial. The influence of such domains on the gluonic energy density is studied.

Keywords: Deconfining phase transition; lattice gauge theory; spin systems; dynamical evolution, spinodal decomposition.

1. Introduction

In Ref. 1, 2 it is emphasized that in studies of the QCD deconfining transition (or cross-over) by means of heavy ion experiments, one ought to be concerned about non-equilibrium effects after a rapid *heating* of the system. This is because the heating may be modelled as a rapid quench and the QCD high temperature vacuum is characterized by ordered Polyakov loops which are similar to the low temperature phase of analogue spin models. The subsequent evolution leads to vacuum domains of distinct Z_3 triality, and one ought to be concerned about non-equilibrium effects.

Here we extend the investigation to SU(3) lattice gauge theory. We report preliminary results about the influence of such domains on the gluonic energy density and pressure of pure SU(3) lattice gauge theory.

The Markov chain Monte Carlo (MC) process provides model A (Glauber) dynamics in the classification of Ref. 3. As a time step a sweep of systematic updating

*Present address: Department of Physics and Astronomy, University of California, Los Angeles, CA 90095-1547, USA with the Cabibbo-Marinari [4] heat-bath algorithm and its improvements of Ref. 5, 6 is used (no over-relaxation, to stay in the universality class of Glauber dynamics). Although this is certainly not the physical dynamics of QCD, in the present state of affairs it appears important to collect qualitative ideas about eventual dynamical effects. For this purpose the investigation of any dynamics, which actually allows for its study ought to be useful.

2. Preliminaries

2.1. *Two-Point Correlation Function*

Consider two-point correlation functions defined by

$$\langle u_0(0) u_0^\dagger(\vec{j})\rangle_L = \frac{1}{N_\sigma^3} \sum_{\vec{i}} u_0(\vec{i}) u_0^\dagger(\vec{i}+\vec{j}), \tag{1}$$

where $u_0(\vec{i})$ is the relevant fluctuation about some average and $\vec{i}$ denotes spatial coordinates. Periodic boundary conditions are used and the subscript L on the left-hand side reminds us that the average is taken over the spatial lattice. For gauge systems we deal with fluctuations of the Polyakov loop, and for analogue spin systems with fluctuations of the magnetization.

The finite volume continuum limit of (1) is achieved by lattice spacing $a \to 0$, $N_\sigma \to \infty$ with the physical length of the box $L = aN_\sigma = const$. This means that

$$\langle u_0(0) u_0^\dagger(\vec{j})\rangle_L = \frac{1}{a^3 N_\sigma^3} \sum_{\vec{i}} a^3 u_0(\vec{i}) u_0^\dagger(\vec{i}+\vec{j}) \tag{2}$$

transforms into

$$\langle u(0) u^\dagger(\vec{R})\rangle_L = \frac{1}{L^3} \int d^3r\, u(\vec{r}) u^\dagger(\vec{r}+\vec{R}), \tag{3}$$

with $\vec{r} = a\vec{i}$, $\vec{R} = a\vec{j}$, $u(\vec{r}) = u_0(\vec{i})$, and so on.

2.2. *Structure Functions*

We define structure function as Fourier transform of the two-point correlation function (3):

$$F(\vec{p}) = \int \langle u(0) u^\dagger(\vec{R})\rangle_L \, e^{i\,\vec{p}\,\vec{R}}\, d^3R. \tag{4}$$

Occasionally it is also convenient to use structure functions normalized by the volume:

$$S(\vec{p}) = \frac{1}{L^3} \int \langle u(0) u^\dagger(\vec{R})\rangle_L \, e^{i\,\vec{p}\,\vec{R}}\, d^3R. \tag{5}$$

Periodic boundary conditions imply:

$$\vec{p} = \frac{2\pi}{L}\vec{n}, \tag{6}$$

where $\vec{n}$ is an integer vector $(0,0,0)$, $(0,0,1)$, etc.

The discretized version of (4) is

$$F(\vec{p}) = \sum_{\vec{j}} a^3 \, \langle u_0(0) u_0^\dagger(\vec{j}) \rangle_L \, e^{i\,a\,\vec{p}\,\vec{j}}. \tag{7}$$

Using definition (1) and shifting summation on $\vec{j}$ one arrives (after simple algebra) at the expression

$$F(\vec{p}) = \frac{a^3}{N_\sigma^3} \left| \sum_{\vec{i}} e^{-i\,a\,\vec{p}\,\vec{i}} \, u_0(\,\vec{i}\,) \right|^2 . \tag{8}$$

Rewriting the product in the exponent as

$$a\,\vec{p}\,\vec{i} \,=\, a\,\frac{2\pi}{L}\,\vec{n}\,\vec{i} \,=\, a\,\frac{2\pi}{aN_\sigma}\,\vec{n}\,\vec{i} \,=\, \frac{2\pi}{N_\sigma}\,\vec{n}\,\vec{i}. \tag{9}$$

and using definition (5) we shape $S(\vec{p})$ into the form used in our simulations:

$$S(\vec{p}) = \left| \frac{1}{N_\sigma^3} \sum_{\vec{i}} \exp\left\{ -\frac{2\pi i}{N_\sigma}\,\vec{n}\,\vec{i} \right\} u_0(\,\vec{i}\,) \right|^2 . \tag{10}$$

As we let system evolve with time quantity $u_0(\vec{i})$ becomes time-dependent: $u_0(\vec{i},t)$. The time t corresponds to the dynamical process, i.e., in our case the Markov chain MC time. We consider an ensemble of systems (replica) and dynamical observables are calculated as ensemble averages denoted as $\langle ... \rangle$. Then time-dependent structure functions averaged over replicas are:

$$\hat{S}(\vec{p},t) = \langle S(\vec{p},t) \rangle = \left\langle \left| \frac{1}{N_\sigma^3} \sum_{\vec{i}} \exp\left\{ -\frac{2\pi i}{N_\sigma}\,\vec{n}\,\vec{i} \right\} u_0(\vec{i},t) \right|^2 \right\rangle . \tag{11}$$

Similarly,

$$\hat{F}(\vec{p},t) = L^3 \hat{S}(\vec{p},t). \tag{12}$$

Early time evolution of the structure functions after the quench is governed by the linear theory. The linear approximation results in the following equation for the structure function:

$$\frac{\partial \hat{S}(\vec{p},t)}{\partial t} = 2\,\omega(\vec{p})\,\hat{S}(\vec{p},t)\,, \tag{13}$$

with the solution

$$\hat{S}(\vec{p},t) \;=\; \hat{S}(\vec{p},t=0)\exp\left(2\omega(\vec{p})t\right)\,, \qquad \omega(\vec{p}) > 0 \;\text{ for }\; |\vec{p}| > p_c\,, \tag{14}$$

where $p_c > 0$ is a critical momentum. Originally the linear theory was developed for model B [7,8]. Details for model A can be found in Ref. 2.

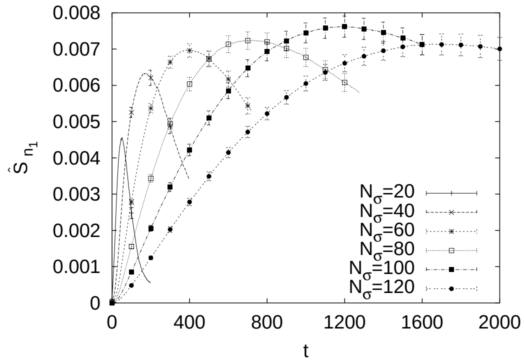

Fig. 1. The first structure function mode for the 3D 3-state Potts model on N_σ^3 lattices.

During our simulations the structure functions are averaged over rotationally equivalent momenta and the notation $\hat{S}_{n_i}$ is used for the structure function at momentum

$$\vec{p} = \frac{2\pi}{L}\,\vec{n} \quad \text{where} \quad |\vec{n}| = n_i\,. \tag{15}$$

The $\hat{S}_{n_i}$ are called structure function modes or structure factors. We recorded the modes (including the permutations) n_1: $(1,0,0)$, n_2: $(1,1,0)$, n_3: $(1,1,1)$, n_4: $(2,0,0)$, n_5: $(2,1,0)$, n_6: $(2,1,1)$, n_7: $(2,2,0)$, n_8: $(2,2,1)$ and $(3,0,0)$, n_9: $(3,1,0)$, n_{10}: $(3,1,1)$, n_{11}: $(2,2,2)$, n_{12}: $(3,2,0)$, n_{13}: $(3,2,1)$, n_{14}: $(3,2,2)$, n_{15}: $(3,3,0)$, n_{16}: $(3,3,1)$, n_{17}: $(3,3,2)$, n_{18}: $(3,3,3)$. Note that there is an accidental degeneracy in length for n_8.

3. Numerical Results

3.1. *Structure Function Modes*

In Figs. 1, 2, 3 the time evolution of the first structure function mode $\hat{S}_{n_1}$ after a heating quench is depicted (from $\beta = 0.2 \to 0.3$ in the 3D 3-state Potts model, from $\beta = 2.0 \to 3.0$ in pure SU(2) and from $\beta = 5.5 \to 5.92$ in pure SU(3) lattice gauge theory). Notable in these figures is the strong increase of the maxima $\hat{S}_{n_1}^{\max}$ with lattice size. In our normalization of $\hat{S}_{n_1}$ non-critical behavior corresponds to a fall-off $\sim 1/N_\sigma^3$ and a second order phase transition to a slower fall-off $\sim 1/N_\sigma^x$ with $0 < x < 3$. As the $N_\sigma \to \infty$ limit is bounded by a constant, our figures show that with our lattice sizes the asymptotic behavior may have been reached for the 3D 3-state Potts model and for SU(2), but not yet for SU(3) lattice gauge theory.

Our Potts results are from Ref. 2. Our results for SU(2) are averages over 10,000 repetitions for the 4×16^3 lattice, 4,000 for 4×32^3, 800 for 4×48^3, 340 for 4×64^3 and 106 for the 4×80^3 lattice. For SU(3) we rely on 10,000 repetitions of the quench for the 4×16^3 lattice, 4,000 for 4×32^3 and 170 for the 4×64^3 lattice.

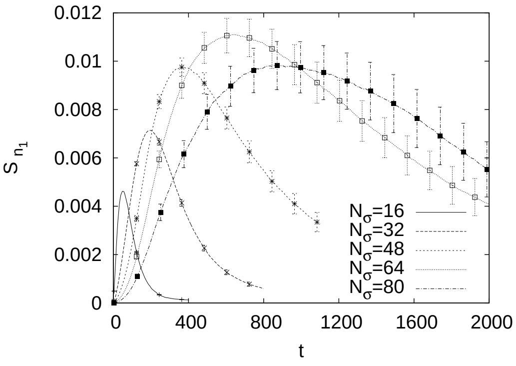

Fig. 2. The first structure function mode for pure SU(2) lattice gauge theory on $4 \times N_\sigma^3$ lattices.

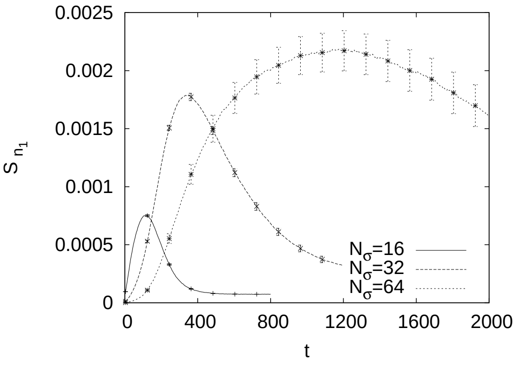

Fig. 3. The first structure function mode for pure SU(3) lattice gauge theory on $4 \times N_\sigma^3$ lattices.

The results [2] of $\omega(k)$ fits from a $\beta = 0.2 \to 0.3$ quench at zero external magnetic field in the 3D 3-state Potts model are compiled in Fig. 4 versus n^2/N_σ^2. Approximately, we find straight lines $\omega(k) = a_0 + a_1\, n^2$ with a negative slope a_1 and we determine the critical momentum $k_c = 2\pi\, n_c/N_\sigma$ as the value where $\omega(k)$ changes its sign. We find $k_c \approx 0.349$ from our combined data taken on the 40^3, 80^3 and 100^3 lattices [18].

We use the same techniques to determine the critical mode p_c in pure SU(3) lattice gauge theory. The results are shown in Fig. 5 and indicate $a\, p_c = k_c = 2\pi\, n_c/N_\sigma \approx 0.34$ (from the figure $n_c^2/N_\sigma^2 \approx 0.003$). Relying on a phenomenological analysis by Miller and Ogilvie [10], p_c is related by $m_D = \sqrt{3}\, p_c$ to the Debye screening mass at the final temperature T_f after the quench. The relation $k_c/T_f = N_\tau\, a\, k_c$ determines T_f and allows us to convert m_D to physical units. For our quench we have $T_f/T_c = 1.57$ and get

$$m_D = \sqrt{3}\, N_\tau\, a\, k_c\, T_f = 3.7\, T_c \; . \tag{16}$$

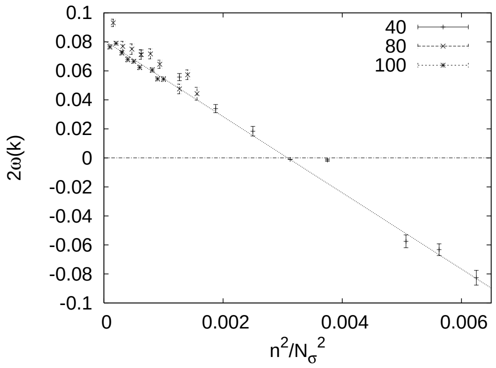

Fig. 4. Determination of k_c for the 3D 3-state Potts model on N_σ^3 lattices.

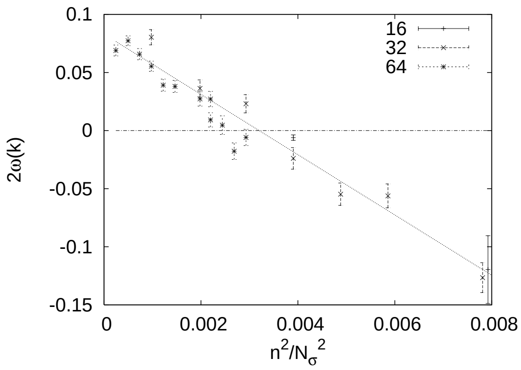

Fig. 5. Determination of k_c for the pure SU(3) lattice gauge theory on $4 \times N_\sigma^3$ lattices.

For pure SU(3) lattice gauge theory $T_c = 265\,(1)\,\mathrm{MeV}$ holds, assuming $\sigma = 420\,\mathrm{MeV}$ for the string tension, while for QCD the cross-over temperature appears to be around $T_c \approx 165\,\mathrm{MeV}$, see Ref. 13 for a recent review.

In Fig. 3 we observe that not only the heights of the peaks increases with the spatial volume, but also the time $t_{\max}$, $\hat{S}^{\max}_{n_1} = \hat{S}_{n_1}(t_{\max})$, which it takes to reach them. Whereas $\hat{S}^{\max}_{n_1}$ has finally to approach a constant value, $t_{\max}$ is expected to diverge with lattice size due to the competition of vacuum domain of distinct Z_3 triality.

For the Potts models the Fortuin-Kasteleyn (FK) cluster definition can be used to exactly remap the phase transition into a percolation model. In case of the 3D 3-state Potts model the states substitute for the Z_3 trialities of SU(3) lattice gauge theory. In the cluster language the competition of distinct vacuum domains can be made visible [2]. In Fig. 6 we compare the evolution of geometrical and FK clusters for a quench of the 3D 3-state Potts model from its disordered into its ordered phase.

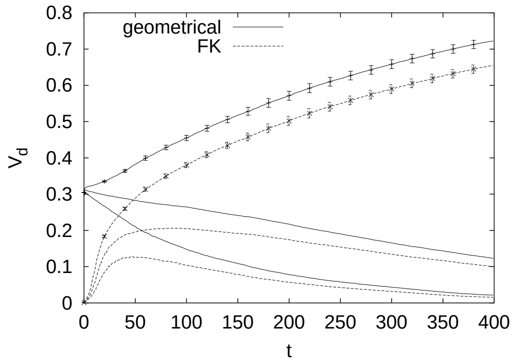

Fig. 6. Largest geometrical and FK clusters for the 3D 3-state Potts model quenched from $\beta = 0.2$ to $\beta_f = 0.3$ on a 40^3 lattice.

We plot the evolution of the largest clusters for the three Potts magnetizations in zero external magnetic field h. While the system grows competing FK clusters of each magnetization before one becomes dominant, geometrical clusters do not compete. This picture is unfavorable for the use of geometrical clusters of Polyakov loops in gauge theories, for which the FK definition does not exist.

The process of competitions between the largest FK clusters of different magnetization leads for the proper transition ($h = 0$) to a divergence of the equilibration time in the limit of infinite systems, an effect known in condensed matter physics [3]. Potts studies [2] with an external magnetic field show that a major slowing down effect survives when $h \neq 0$ is sufficiently small. As the influence of an external magnetic field on the Potts model is similar to that of quarks on SU(3) gauge theory this indicates that the effect may be of relevance for QCD studies of the crossover region.

3.2. *Gluonic Energy Density*

Although a satisfactory cluster definition does not exist for gauge theories, the underlying mechanism of competing vacuum domains is expected to be similar as in the spin models. To study its influence on the gluonic energy ϵ and pressure p densities, we calculate these quantities at times $t \leq t_{\max}$.

The equilibrium procedure is summarized in Ref. 9, 11 (in earlier work [12,15] the pressure exhibited a non-physical behavior after the deconfining transition and the energy density approached the ideal gas limit too quickly because the anisotropy coefficients were calculated perturbatively). We denote expectation values of space-like plaquettes by P_σ and those involving one time link by P_τ. The energy density and pressure can then be cast into the form

$$(\epsilon + p)/T^4 = 8N_cN_\tau^4 g^{-2}\left[1 - \frac{g^2}{2}[c_\sigma(a) - c_\tau(a)]\right](P_\sigma - P_\tau) \tag{17}$$

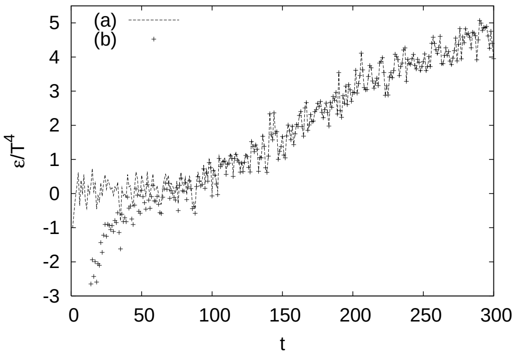

Fig. 7. SU(3) gluonic energy density: (a) with P_0 calculated from the time series after the quench and (b) using equilibrium values for P_0.

and

$$(\epsilon - 3p)/T^4 = 12 N_c N_\tau^4 \left[c_\sigma(a) - c_\tau(a)\right] \left[2P_0 - (P_\sigma + P_\tau)\right], \tag{18}$$

where P_0 is the plaquette expectation value on a symmetric ($T = 0$) lattice, and the *anisotropy coefficients* $c_{\sigma,\tau}(a)$ are defined by:

$$c_{\sigma,\tau}(a) \equiv \left(\frac{\partial g_{\sigma,\tau}^{-2}}{\partial \xi}\right)_{\xi=1}. \tag{19}$$

They are related to the QCD β-function and can be calculated using Pade fits of Ref. 9. As was shown in Ref. 14 this procedure can be successfully used for the quench. To normalize to zero temperature, plaquette values from the symmetric $N_\tau = N_\sigma$ lattice are needed in Eq. (18). As one stays within the confined phase on the symmetric lattice its equilibration after the quench is fast. Therefore it is enough to use equilibrium values of P_0 (at final $\beta_f = 5.92$) after the quench. This is illustrated in Fig. 7.

In Fig. 8 we report how the time needed for equilibration increases with lattice size. We compare the evolution of the gluonic energy density on lattices 4×16^3, 4×32^3 and 4×64^3. A slowing down of the equilibration is found, which appears to be related to the divergence of the time needed to reach the structure factor maxima.

Finally, we compare in Fig. 9 for the $N_\sigma = 16$ lattice the gluonic energy distribution in equilibrium at $\beta = 5.92$ with the one obtained after 148 time steps. We find a shift towards lower gluonic energies and the width of the probability density is slightly broader for the time evolution after the quench than in equilibrium. One also has to take into account that the geometry of relativistic heavy ion experiments experiments is reasonably approximated by $N_\tau/N_\sigma = \text{const}$, $N_\sigma \to \infty$, rather than by $N_\tau = \text{const}$, $N_\sigma \to \infty$.

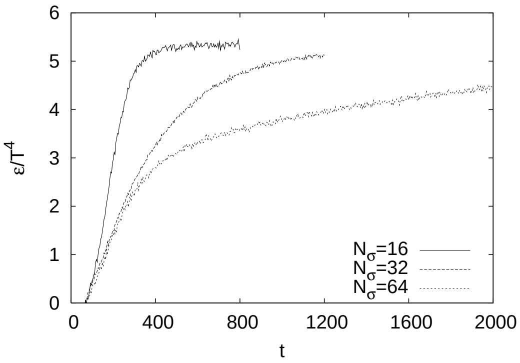

Fig. 8. The time evolution of SU(3) gluonic energy density on $4 \times N_\sigma^3$ lattices.

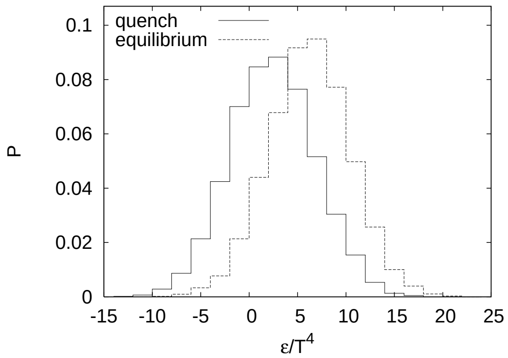

Fig. 9. SU(3) gluonic energy density $P(\epsilon)$ histograms on a 4×16^3 lattice: (a) with competing vacuum domains present and (b) after reaching equilibrium.

4. Summary and Conclusions

Using the evolution of structure function modes, we identify spinodal decomposition as the transition scenario for quench from the disordered into the ordered phase of SU(3) lattice gauge theory and the analogue Potts model. We observe an early time development of structure factors $S_n(t)$, which is in over-all agreement with the exponential growth predicted by the linear theory of spinodal decomposition for $|\vec{p}| < p_c$. From our data the critical mode p_c is estimated. Using phenomenological arguments [10], p_c is used to determine the Debye screening mass m_D at the final temperature T.

With increasing lattice size N_σ the time to reach the structure factor maxima diverges. Relying on a study of Fortuin-Kasteleyn clusters in Potts models [2], we assume that the reason for the slowing down is due to competing vacuum domains. For SU(3) gauge theory these are domains of distinct Z_3 trialities. They may be the relevant vacuum configurations after the heating quench in relativistic heavy ion collision experiments. We have initiated a study of the gluonic energy and pressure densities on such configurations. Our data are consistent with a divergence of the equilibration time of the gluonic energy density, similarly to the one observed for the structure factor maxima.

All our results rely on using a dissipative, non-relativistic time evolution, believed to be in the Glauber universality class. The hope is that the thus created non-equilibrium configurations may exhibit some features, which are in any dynamics typical for the state of the system after the quench. This hope could get more credible by studying a Minkowskian time evolution of Polyakov loops and finding similar features. Such a study appears to be possible [16] within a relativistic Polyakov loop model which was introduced by Pisarski [17].

Acknowledgments

This work was in part supported by the US Department of Energy under contract DE-FG02-97ER41022. The simulations were performed on PC clusters at FSU.

References

1. B.A. Berg, U.M. Heller, H. Meyer-Ortmanns, and A. Velytsky, *Phys. Rev.* **D69**, 034501 (2004).
2. B.A. Berg, H. Meyer-Ortmanns, and A. Velytsky, *Phys. Rev.* **D70**, 054505 (2004).
3. P.M. Chaikin and T.C. Lubensky, *Principles of condensed matter physics* (Cambridge University Press, Cambridge, 1997).
4. N. Cabibbo and E. Marinari, it Phys. Lett. **B119**, 387 (1982).
5. K. Fabricius and O. Hahn, *Phys. Lett.* **B143**, 459 (1984).
6. A.D. Kennedy and B.J. Pendleton, *Phys. Lett.* **B156**, 393 (1985).
7. J.W. Cahn and J.E. Hilliard, *J. Chem. Phys.* **28**, 258 (1958).
8. J.W. Cahn, *Trans. Metall. Soc. AIME* **242**, 166 (1968).
9. G. Boyd, J. Engels, F. Karsch, E. Laermann, C. Legeland, M. Lütgemeier, and B. Peterson, *Nucl. Phys.* **B469**, 419 (1996).
10. T.R. Miller and M.C. Ogilvie, *Nucl. Phys. (Proc. Suppl.)* **B106**, 537 (2002); *Phys. Lett.* **B488**, 313 (2000).
11. J. Engels, F. Karsch, and T. Scheideler, *Nucl. Phys.* **B564**, 303 (2000).
12. Y. Deng, *Nucl. Phys. (Proc. Suppl.)* **9**, 334 (1989).
13. P. Petreczky, *hep-lat/0409139*.
14. A. Bazavov, B.A. Berg and A. Velytsky, *hep-lat/0410019*.
15. J. Engels, J. Fingberg, F. Karsch, D. Miller, and M. Weber, *Nucl. Phys.* **B252**, 625 (1990).
16. O. Scavenius, A. Dumitru and A.D. Jackson, *Phys. Rev. Lett.* **87**, 182302 (2001).
17. R.D. Pisarski, *Phys. Rev.* **D62**, 111501(R) (2000); A. Dumitru and R. Pisarski, *Phys. Lett.* **B504**, 282 (2001).
18. A. Velytsky, PhD thesis, Florida State University, 2004.